Cell Death and Differentiation (2013) 20, 218–225

www.nature.com/cdd

Identification of factors that function in *Drosophila* salivary gland cell death during development using proteomics

CK McPhee[1,2,3], BM Balgley[4], C Nelson[1], JH Hill[1,2,5], Y Batlevi[1], X Fang[6], CS Lee[6] and EH Baehrecke*,[1]

Proteasome inhibitors induce cell death and are used in cancer therapy, but little is known about the relationship between proteasome impairment and cell death under normal physiological conditions. Here, we investigate the relationship between proteasome function and larval salivary gland cell death during development in *Drosophila*. *Drosophila* larval salivary gland cells undergo synchronized programmed cell death requiring both caspases and autophagy (*Atg*) genes during development. Here, we show that ubiquitin proteasome system (UPS) function is reduced during normal salivary gland cell death, and that ectopic proteasome impairment in salivary gland cells leads to early DNA fragmentation and salivary gland condensation *in vivo*. Shotgun proteomic analyses of purified dying salivary glands identified the UPS as the top category of proteins enriched, suggesting a possible compensatory induction of these factors to maintain proteolysis during cell death. We compared the proteome following ectopic proteasome impairment to the proteome during developmental cell death in salivary gland cells. Proteins that were enriched in both populations of cells were screened for their function in salivary gland degradation using RNAi knockdown. We identified several factors, including *trol*, a novel gene *CG11880*, and the cop9 signalsome component *cop9 signalsome 6,* as required for *Drosophila* larval salivary gland degradation.
Cell Death and Differentiation (2013) **20,** 218–225; doi:10.1038/cdd.2012.110; published online 31 August 2012

Programmed cell death is critical to multi-cellular animal development and homeostasis, and misregulation of cell death can lead to disorders including autoimmunity and cancer.[1–3] Three prominent morphological forms of programmed cell death occur during development, including apoptosis, programmed necrosis, and autophagic cell death.[4,5] Autophagic cell death is characterized by the induction of autophagy in dying cells that are degraded and removed without known phagocytic uptake.[4] Although our understanding of autophagic cell death has recently increased, how autophagy and other catabolic processes promote cell death and degradation remains poorly understood.

Cells use two general catabolic processes to degrade and recycle cellular components, the ubiquitin proteasome system (UPS) and autophagy. During autophagy, cytoplasmic contents are sequestered by the autophagosome and delivered to the lysosome for degradation. Proteins to be degraded by the UPS are polyubiquitinated and targeted to the proteasome, an ATP-dependent 26S multisubunit protease complex.[6] Whereas the UPS is used to degrade short-lived proteins, autophagy is generally thought to degrade long-lived proteins. Although the fundamental processes of autophagy and the UPS are understood, less is known about the function of these processes during programmed cell death.

The UPS has a key role in multiple cellular processes, including cell cycle regulation[7] and antigen processing.[8] Studies have also suggested a role for the UPS in coordinating cell death.[9] Studies in cell lines suggest that caspase-dependent proteasome impairment may facilitate cell death.[10,11] Furthermore, changes in ubiquitination and proteasome composition occur during hawkmoth development in dying intersegmental muscle cells.[12–15] Interestingly, these cells die with autophagic cell death morphology, suggesting a possible role for the UPS in autophagic cell death, but this has not been tested empirically.

Several studies suggest that ectopic proteasome impairment induces cell death in cell lines,[16,17] and drug-induced proteasome impairment in tumor cells results in caspase activation and cell death.[18] In addition, proteasome inhibitors are used in cancer therapies.[19] The reversible proteasome inhibitor Bortezomib (Velcade, Millennium Parmaceuticals, Cambridge, MA, USA) is used to treat myeloma and lymphoma.[20] Evidence in cell lines suggests that proteasome inhibitors lead to cell death by downregulating NF-κB signaling[21,22] and/or by inducing endoplasmic-reticulum stress.[23,24] However, little is known about the effects of proteasome inhibitors on cellular processes, and how proteasome inhibition leads to cell death

[1]Department of Cancer Biology, University of Massachusetts Medical School, Worcester, MA 01605, USA; [2]Department of Cell Biology and Molecular Genetics, University of Maryland, College Park, MD 20742, USA; [3]Department of Molecular and Cellular Biology, Harvard University, Cambridge, MA 02138, USA; [4]Bioproximity LLC, Springfield, VA 22150, USA; [5]Laboratory of Molecular Genetics, National Heart, Lung, and Blood Institute, National Institutes of Health, Bethesda, MD 20892, USA and [6]Department of Chemistry and Biochemistry, University of Maryland, College Park, MD 20742, USA
*Corresponding author: EH Baehrecke, Department of Cancer Biology, University of Massachusetts Medical School, Lazare Research Building, Room 423, Worcester, MA 01605, USA. Tel: 508 856 6733; Fax: 508 856 1310; E-mail: Eric.Baehrecke@umassmed.edu
Keywords: autophagy; programmed cell death; ubiquitin proteasome system; proteomics; cop9 signalsome; trol/perlecan
Abbreviations: UPS, ubiquitin proteasome system; MS, mass spectrometry; CSN6, cop9 signalsome 6
Received 9.1.12; revised 30.6.12; accepted 10.7.12; Edited by RA Knight; published online 31.8.12

has not been investigated under physiological conditions *in vivo*.

Larval salivary gland cells undergo synchronized programmed cell death requiring both caspases and autophagy (*Atg*) genes during *Drosophila* development.[25] In wild-type *Drosophila*, the onset of salivary gland cell death occurs 12 h after puparium formation (APF), and DNA fragmentation and caspase activity can be detected at this time. Between 13 and 14 h APF, autophagy is induced and salivary glands become smaller in size, or condensed. By 16 h APF, wild-type salivary glands are completely degraded.

Recent developments in high-throughput mass spectrometry (MS)-based proteomic technologies prompted us to conduct a new proteomic analysis of dying salivary glands in *Drosophila*. We found that among the groups of proteins identified, UPS components were the top category enriched in wild-type dying salivary glands, suggesting a possible role for the UPS in larval salivary gland cell death. We monitored UPS function in salivary gland cells and found that flux through the UPS is reduced during wild-type salivary gland cell death. Significantly, premature proteasome impairment using an inducible genetic proteasome mutant leads to the onset of early salivary gland condensation (an overall reduction in salivary gland size) and DNA fragmentation, as evidenced by TUNEL staining. Surprisingly, we find that the expression of the caspase inhibitor p35 during proteasome impairment does not suppress early salivary gland condensation. This suggests the involvement of caspase-independent factors in the cellular response to proteasome impairment leading to ectopic salivary gland condensation. To identify factors that function in the response to proteasome impairment during autophagic cell death, we conducted proteomic analyses of salivary glands following ectopic proteasome impairment. We used a genetic approach to screen the top candidates identified in our proteomics data sets for defects in salivary gland degradation. Here, we show that *trol*, *CG11880*, a gene of unknown function, and the cop9 signalsome component *csn6,* are required for salivary gland cell degradation.

Results

UPS components are enriched in dying *Drosophila* larval salivary glands. During *Drosophila* development, autophagic programmed cell death of larval salivary glands is triggered by a rise in the steroid hormone 20-hydroxyecdysone (ecdysone) 12 h after APF, and requires both caspases and autophagy.[25–27] In wild-type animals, salivary glands begin to die 12 h APF, and DNA degradation and caspase activation can be detected at this time in salivary gland cells. By 13–14 h APF, autophagy is induced and salivary glands become smaller in size, or condensed. Thereafter, salivary glands are rapidly degraded and are absent by 16 h APF.

To identify new proteins required for larval salivary gland cell degradation, we isolated proteins from purified larval salivary glands before (6 h APF), during (12 h APF), and after (13.5 h APF) the onset of salivary gland cell death (Supplementary Table S1). In the 6-h samples, we identified an average of 12 487 distinct peptides that mapped to 4157 distinct proteins with $>95\%$ confidence (Supplementary Table S2). Similarly, in the 12-h samples, we identified an average of 11 530 distinct peptides that mapped to 3566 distinct proteins, and in the 13.5-h samples, we identified an average of 13 012 distinct peptides that mapped to an average of 4184 distinct proteins with $>95\%$ confidence (Supplementary Table S2).

Using this proteomic approach, proteins previously shown to be involved in salivary gland programmed cell death were identified, including the ecdysone receptor component Usp, the ecdysone response protein Eip93F (E93), the nuclear receptor competence factor βFtz-f1, the *Drosophila* caspase protease Ice (DrIce), and several autophagy proteins (Supplementary Table S3). These data are consistent with published DNA microarray and proteomics studies,[28,29] as well as genetic studies showing that these factors are required for salivary gland cell death.[25,27,30,31]

We sought to identify groups of proteins that were enriched in dying salivary glands that might suggest the involvement of either a cellular process or a genetic pathway in salivary gland cell death. We used Ingenuity Pathway Analysis to analyze the 6-, 12-, and 13.5-h proteomics data sets, and this approach identified the protein ubiquitination pathway as the top category enriched in dying salivary glands. In two-way comparisons, we identified groups of proteins that increased in detection values between 6 and 13.5 h APF (Supplementary Table S4). The enrichment of a large number of proteasome components and ubiquitination regulators in dying salivary glands suggested a possible role for the UPS in salivary gland cell death (Table 1). These findings suggest several possibilities; UPS components may be enriched in dying salivary glands because the UPS has an increased function during salivary gland cell death. Alternatively, if the UPS has reduced function during cell death, it is possible that dying salivary gland cells attempt to compensate by increasing the levels of UPS components.

UPS function is reduced in dying salivary gland cells. Previous studies in cell lines suggest that inhibition of proteasome function may be part of a normal cell death program.[10,11] To monitor UPS function during *Drosophila* salivary gland cell death, we used transgenic fly lines containing UPS reporter substrates that consist of fusions between GFP and degron sequences that target proteins for degradation by the UPS.[32–34] During proper UPS function, GFP is targeted to the proteasome for degradation, whereas GFP accumulates during decreased flux through the UPS pathway.

The GFP reporter for flux through the UPS pathway (UAS-GFP-CL1) was expressed specifically in the salivary glands of experimental animals using the salivary gland-specific driver *forkhead*-GAL4 (*fkh*-GAL4), whereas a stable GFP reporter (UAS-Ub-MGFP) was expressed in salivary glands of control animals. To monitor UPS function in salivary gland cells, glands were dissected and examined by fluorescence microscopy to assay for GFP fluorescence at stages before (6 h APF), during (12 h APF), and after the onset of salivary gland cell death (13.5 h APF). All of the control animals possess fluorescence in salivary gland cells 6, 12, and 13.5 h APF (Figure 1a, top panels). Salivary glands expressing the UPS flux reporter GFP-CL1 exhibit low fluorescence at 6 and

Table 1 List of UPS components enriched in dying wild-type *Drosophila* larval salivary glands

		Wild-type 6 *versus* 13.5 h	
Symbol	**Notes**	**Ratio2**	***P*-value**
ari-1	Ubiquitin-protein ligase activity	1.5	0.7884
CG17331	Proteasome core complex	1.1	0.5807
CG1950	Ubiquitin thiolesterase activity	1.5	0.4562
CG30382	Proteasome core complex	1.2	0.5712
CG3473	Ubiquitin-protein ligase activity	1.2	0.9195
CG7656	Ubiquitin-protein ligase activity	1.1	0.9309
CG8184	Ubiquitin-protein ligase activity	Inf	0.2855
CG9086	Ubiquitin-protein ligase activity	5.9	0.0651
crl	Ubiquitin-protein ligase activity	Inf	0.2855
Cul-2	Ubiquitin-protein ligase binding	1.2	0.9108
Cul-2	Ubiquitin-protein ligase binding	1.2	0.9108
Cul-5	Cullin-RING ubiquitin ligase complex	1.5	0.7994
hyd	Ubiquitin-protein ligase activity	1.1	0.9309
Pros25	Proteasome core complex	1.5	0.0136
Pros26.4	Proteasome regulatory particle	1.1	0.5846
Pros45	Proteasome regulatory particle, base subcomplex	1.3	0.1907
Prosalpha3T	Endopeptidase activity	1.2	0.9195
Prosalpha5	Proteasome complex	1.1	0.4613
Prosbeta1	Proteasome core complex	1.3	0.0064
Prosbeta3	Proteasome core complex	1.3	0.1033
Prosbeta7	Proteasome core complex	1.1	0.523
Prp19	Ubiquitin-protein ligase activity	7.2	0.02349
Rpn1	Proteasome regulatory particle, base subcomplex	1.5	0.0088
Rpn11	Proteasome regulatory particle, lid subcomplex	1.1	0.5851
Rpn2	Proteasome regulatory particle, base subcomplex	1.4	0.011
Rpn5	Proteasome regulatory particle, lid subcomplex	1.5	0.05447
Rpn7	Proteasome regulatory particle, lid subcomplex	1.3	0.4598
slmb	Ubiquitin-protein ligase activity	Inf	0.2855
Tbp-1	Proteasome regulatory particle	1.6	0.03149
UbcD4	Ubiquitin-protein ligase activity	Inf	0.2855
UbcD6	Ubiquitin-protein ligase activity	1.2	0.8294
Ubc-E2H	Ubiquitin-protein ligase activity	1.1	0.9407
Ufd1 like	Proteasome complex, base subcomplex	2.4	0.4157

Abbreviations: Inf, a numerical value divided by 0. –Inf, 0 divided by a numerical value; UPS, ubiquitin proteasome system.
Protein names are based on Flybase annotation (http://flybase.org/). The ratio2 values for peptides mapped to the genes listed are indicated (ratio2 = average detection value in the 13.5-h sample divided by average detection value in the 6-h sample). *P*-values were obtained using the Student's *t*-test followed by multiple testing adjustment using the Benjamini–Hochberg method.[51]

12 h APF (Figure 1a, bottom panels). However, GFP fluorescence increases dramatically in salivary glands by 13.5 h APF (Figure 1a, bottom panels), suggesting that flux through the UPS pathway is decreased in dying salivary glands, perhaps due to a decrease in UPS function. If UPS function is decreased in salivary gland cells during cell death, we would expect ubiquitinated proteins to accumulate in these cells. We analyzed wild-type salivary gland protein extracts by western blot with ubiquitin antibody and found that ubiquitinated proteins increase in salivary gland extracts between 6 and 13.5 h APF (Figure 1b). These results suggest that the flux through the UPS pathway decreases, and the function of the UPS is reduced, during salivary gland cell death.

Ectopic proteasome impairment leads to early salivary gland condensation and DNA fragmentation that is not suppressed by caspase inhibitor p35 expression. Proteasome impairment leads to caspase activation and cell death in cell lines.[18] To test whether proteasome impairment leads to early cell death *in vivo*, we expressed an inducible dominant temperature-sensitive mutant allele of the β2 subunit of the 20S proteasome (UAS-Dts7^{2c})[35] specifically in salivary gland cells, using the salivary gland-specific GAL4 driver *fkh*-GAL4. To impair proteasome function before the onset of salivary gland cell death, animals expressing Dts7^{2c} in salivary gland cells were shifted from permissive to restrictive temperature at puparium formation (0 h) to 8 h APF. In wild-type animals, salivary gland cell death commences 12 h APF. As a normal aspect of salivary gland cell death, we observe salivary gland condensation, or a decrease in salivary gland size, at 13–14 h APF. Salivary gland condensation can be measured as a decrease in salivary gland area in histological sections. We found that salivary glands of control animals lacking the GAL4 driver (UAS-Dts7/+) are intact and have a normal size and morphology at 8 h APF. In contrast, we observed that salivary glands of experimental animals, in which the proteasome is ectopically impaired specifically in salivary gland cells (*fkh*-GAL4/+; UAS-Dts7^{2c}/+), are smaller in size, or more condensed, than those of control animals (Figure 2a). To quantify salivary gland size, we measured the area of salivary gland material in histological sections and found a significant difference in salivary gland area between control animals and those with ectopic proteasome impairment in salivary gland cells (Figure 2e). These data suggest that *in vivo* ectopic proteasome impairment

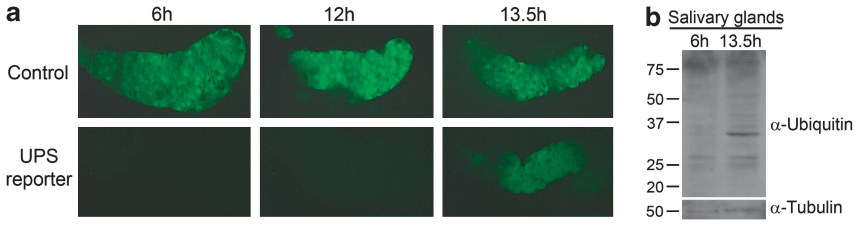

Figure 1 UPS function is reduced during wild-type salivary gland developmental cell death. (**a**) Control animals (*fkh*-GAL4/+; UAS-Ub-M-GFP/+) expressing a stable GFP reporter in salivary glands exhibit GFP fluorescence in salivary glands 6, 12, and 13.5 h AFP, $n=11$. Pupae with salivary gland-specific expression of a GFP reporter for UPS impairment (*fkh*-GAL4/+; UAS-GFP-CL1/+) exhibit low GFP fluorescence in salivary glands at 6 and 12 h AFP, but intense GFP fluorescence in salivary glands 13.5 h AFP, $n=29$. (**b**) Protein extracts from wild-type salivary glands 6 and 13.5 h AFP were analyzed by western blotting with an anti-ubiquitin antibody

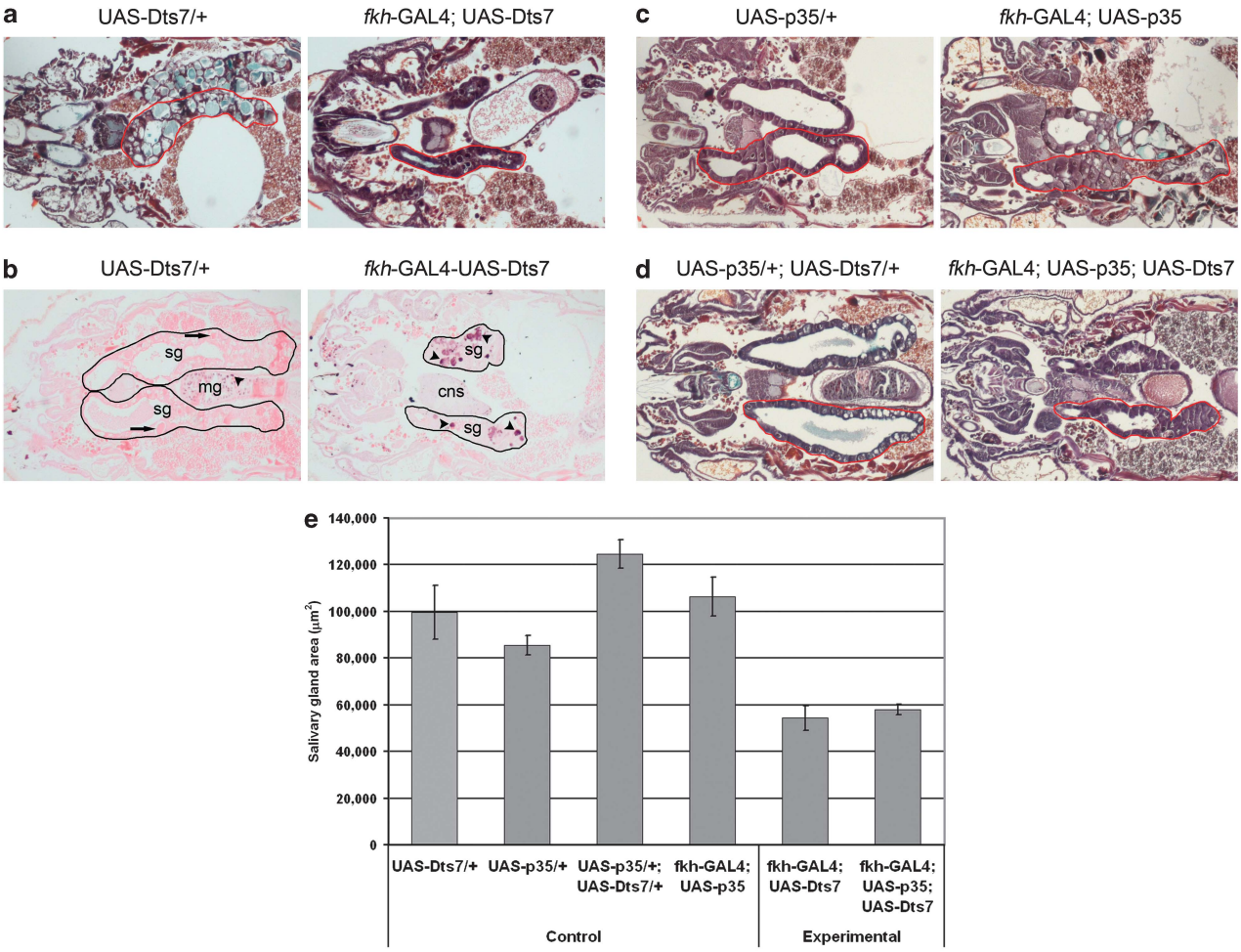

Figure 2 Ectopic proteasome impairment leads to early salivary gland condensation that is not suppressed by caspase inhibitor p35 expression. Pupae were shifted from permissive (25°C) to restrictive (28°C) temperature at puparium formation (0 h), fixed 8 h AFP, and processed for histology. (**a**) Control animals lacking the GAL4 driver (+/UAS-Dts7^{2c}), $n=9$, and those with salivary gland-specific expression of Dts7^{2c} to genetically impair proteasome function (*fkh*-GAL4/+; UAS-Dts7^{2c}/+), $n=13$, were analyzed by histology 8 h after temperature shift for salivary gland material (outlined in red). Gland area is shown in (**e**). (**b**) Control animals (+/UAS-Dts7^{2c}), $n=10$, and those with salivary gland-specific expression of Dts7^{2c} to impair proteasome function (*fkh*-GAL4/+; UAS-Dts7^{2c}/+), $n=12$, were *in situ* TUNEL-labeled to assay for DNA fragmentation. Salivary glands (sg) of control animals lacking the GAL4 driver (+/UAS-Dts7^{2c}) do not possess fragmented DNA, as indicated by light TUNEL-negative salivary gland nuclei (arrows), whereas internal control midgut (mg) nuclei possess fragmented DNA (arrowheads), as indicated by dark TUNEL-positive staining. Salivary glands of experimental animals (*fkh*-GAL4/+; UAS-Dts7^{2c}/+) contain fragmented DNA (arrowheads), as indicated by dark TUNEL-positive staining, following UPS impairment. Cns, central nervous system; mg, midgut; Sg, salivary glands. (**c**) Control animals lacking the GAL4 driver (UAS-p35/+), $n=9$, and those expressing p35 in salivary glands (*fkh*-GAL4/+; UAS-p35/+), $n=18$, were analyzed for salivary gland material (outlined in red). Gland area is shown in (**e**). (**d**) Control animals lacking the GAL4 driver (UAS-p35/+; UAS-Dts7^{2c}/+), $n=12$, and those expressing p35 in the salivary glands (*fkh*-GAL4/+; UAS-p35/+; and UAS-Dts7^{2c}/+), $n=15$, were analyzed for salivary gland material (outlined in red). Gland area is shown in (**e**). (**e**) For all slides of genotypes shown in (**a**, **b**, and **d**), the largest salivary gland section per slide was outlined for measurement, and salivary gland area was measured using the Zeiss AxiovisionLE software. Red outlines designate the area measured. Error bars represent S.E.

in salivary gland cells leads to the early onset of salivary condensation.

We next tested whether ectopic proteasome impairment in salivary gland cells leads to early caspase activation *in vivo*. DNA fragmentation is a caspase-dependent process in salivary glands.[26] We used the TUNEL assay to detect DNA fragmentation in response to ectopic proteasome impairment. Control animals and those expressing Dts7^{2c} in salivary gland cells were shifted from permissive to restrictive temperature at puparium formation (0 h) to 8 h APF, and histological sections were TUNEL stained to assay for DNA fragmentation. We found that whereas the nearby nuclei of the larval midgut of control pupae stain positively for TUNEL at this stage, their salivary gland cells do not (Figure 2b). By contrast, salivary gland cells of pupae expressing Dts7^{2c} contain fragmented DNA as indicated by dark TUNEL-positive salivary gland nuclei (Figure 2b). These data suggest that ectopic proteasome impairment in salivary gland cells leads to early DNA fragmentation *in vivo*.

To test whether the early reduction in salivary gland size upon ectopic proteasome impairment is caspase dependent, we co-expressed the caspase inhibitor p35 with Dts7^{2c} in salivary glands. We found that salivary glands of pupae expressing p35 alone are not significantly different in size compared with control salivary glands (Figures 2c and e). Surprisingly, however, we found that salivary glands of pupae co-expressing p35 and Dts7^{2c} still undergo significant early condensation (Figures 2d and e). These data suggest that although DNA becomes fragmented following ectopic proteasome impairment in salivary gland cells, the early condensation of salivary glands following proteasome impairment may not be caspase-dependent.

Identification of proteins altered following ectopic proteasome impairment that are required for salivary gland degradation. Drugs targeting the proteasome are used in anticancer therapies.[19,20] To better understand cellular responses to altered proteasome function, we conducted a proteomics study of salivary glands following ectopic proteasome impairment. At least three independent biological replicates for each of the control and proteasome impaired salivary gland samples were analyzed using high-throughput shotgun proteomics (Supplementary Table S1). In the proteasome impairment samples (*fkh*-GAL4/+; UAS-Dts7^{2c}/+), an average of 12 601 distinct peptides that mapped to an average of 4184 distinct proteins were identified (Supplementary Table S2). In control samples that lack the GAL4 driver (+/UAS-Dts7^{2c}), an average of 12 094 distinct peptides that mapped to an average of 3922 distinct proteins were identified (Supplementary Table S2). Proteins identified in the proteasome impairment and control samples are listed in Supplementary Table S5. An additional *fkh*-GAL4/+ control was collected and analyzed by proteomics to control for proteins that may be enriched in response to GAL4 expression (data not shown).

We sought to identify genes that are required for salivary gland cell degradation. We queried our proteomics data for proteins that were enriched (indicated by positive ratio2 values) in (1) a two-way comparison between the control (+/UAS-Dts7^{2c}) and ectopic proteasome impairment (*fkh*-GAL4/+; UAS-Dts7^{2c}/+) data sets and also in (2) a two-way comparison between the 6- and 13.5-h APF wild-type dying salivary gland data sets (Supplementary Table S6). Of these, proteins detected in the proteasome impairment sample with *P*-values $\leq$0.002 that were also not previously shown to function in salivary gland degradation were considered top candidates for genetic analyses. From this list of candidate proteins, eight were identified with available transgenic RNAi lines (CG11880, CG3074, CG9336, CG9917, CG9977, Dbi, Ect3, and Trol), and these were all screened for defects in salivary gland cell degradation.

To knockdown genes specifically in salivary gland cells, transgenic fly lines containing UAS-RNAi constructs were crossed to those expressing *fkh*-GAL4. Progeny expressing RNAi in salivary glands were staged to 24 h APF; a stage that is 8 h after salivary gland material is cleared in wild-type *Drosophila*. Of the eight genes tested, two had defects in salivary gland degradation. We found that compared with control animals, those expressing RNAi against the gene encoding Trol possessed persistent salivary gland fragments (Figures 3a and b). Similarly, we found that animals expressing RNAi in salivary glands against *CG11880*, a gene of unknown function, were deficient in salivary gland degradation compared with controls (Figures 3c and d). All other morphological and developmental events occurred normally in these animals, including the timing and morphology of future adult head eversion. Therefore, the inhibition of salivary gland degradation upon either *trol* or *CG11880* expression in salivary glands was not due to a developmental delay. Trol and CG11880 were identified following proteasome inhibition, which follows activation of caspases in salivary glands. As proteasome inhibition can lead to activation of autophagy,[34] we tested if these genes are required for autophagy in dying salivary glands. To our surprise, knockdown of neither *trol* nor *CG11880* had any impact on autophagy (data not shown).To our knowledge, this is the first demonstration that *trol* and *CG1180* are required for salivary gland cell degradation.

The cop9 signalsome (CSN) functions in salivary gland degradation. We queried our proteomics data for proteins that are part of a pathway or cellular process and were enriched both in response to ectopic proteasome impairment and during wild-type salivary gland cell death. Interestingly, the CSN network was identified as being enriched by Ingenuity Pathway Analysis. A number of CSN subunits were detected in both wild-type dying salivary glands and in salivary glands with ectopic proteasome impairment (Table 2). Although the *P*-values for the detection of each individual component were relatively high and therefore did not engender high confidence in the detection of any single subunit, the detection of 7 out of 8 known CSN subunits, including 1b, 3, 4, 5, 6, 7, and 8, suggested a possible role for the CSN in salivary gland death (Table 2).

To test the function of the CSN in salivary gland degradation, we expressed RNAi against the gene encoding CSN subunit 6 (CSN6) in salivary glands. Previous studies have shown that the loss or knockdown of one CSN subunit leads to the destabilization and loss of the entire complex.[36–38] We found that whereas 10% of control animals contained

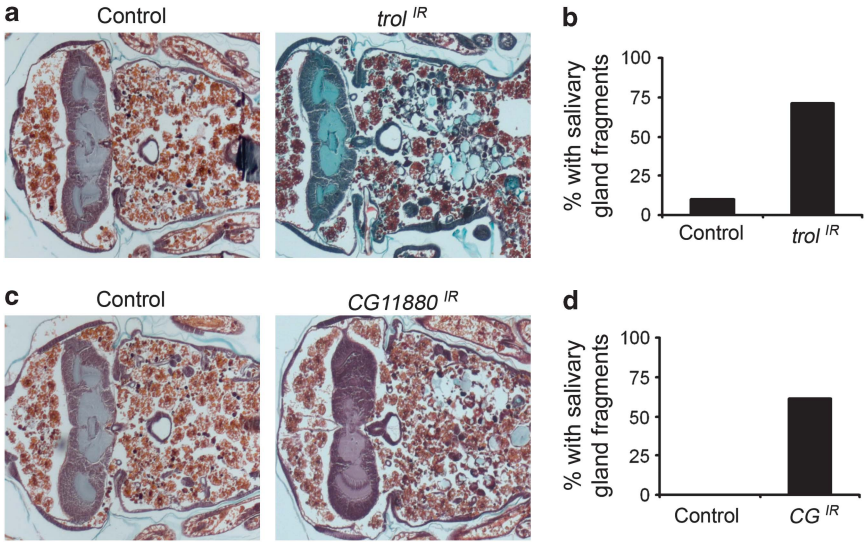

Figure 3 *Trol* and *CG11880* are required for salivary gland cell degradation. (**a**) Control animals lacking the GAL4 driver (+ /w; + /UAS-*trol* ^{IR}), $n = 10$, and those with salivary gland-specific knockdown of trol (*fkh*-GAL4/w; UAS-*trol* ^{IR}/ +), $n = 17$, were analyzed by histology for the presence of salivary glands (red circles) 24 h AFP. (**b**) Quantification of data from (**a**) where 10% of control animals and 71% of experimental animals possess persistent salivary gland fragments. (**c**) Control animals lacking the GAL4 driver (+ /w; + /UAS-*CG11880*^{IR}), $n = 10$, and those with salivary gland-specific knockdown of *CG11880* (*fkh*-GAL4/w; UAS-*CG11880*^{IR}/ +), $n = 23$, were analyzed by histology for the presence of salivary glands (red circles) 24 h AFP. (**d**) Quantification of data from (**c**) where 0% of control animals and 61% of experimental animals possess persistent salivary gland fragments

Table 2 CSN subunits detected in *Drosophila* larval salivary glands by proteomics

		Proteasome impairment		Wild-type 6 *versus* 13.5 h	
Symbol	**Notes**	**Ratio2**	***P*-value**	**Ratio2**	***P*-value**
CSN1b	Signalosome complex subunit 1b	− 1.2	0.7530	Inf	0.2855
CSN3	Signalosome complex subunit 3	− 1.2	0.9047	2.0	0.4593
CSN4	Signalosome complex subunit 4	1.1	0.8339	− 1.6	0.6866
CSN5	Signalosome complex subunit 5	1.6	0.2789	1.8	0.1618
CSN6	Signalosome complex subunit 6	1.8	0.0716	− 2.6	0.4925
CSN7	Signalosome complex subunit 7	1.5	0.2554	4.6	0.2600
CSN8	Signalosome complex subunit 8	− 2.0	0.1428	ND	ND

Abbreviations: CSN, cop9 signalsome; CSN6, cop9 signalsome 6; Inf, a numerical value divided by 0; NA, not applicable; ND, not detected.
Protein names are based on Flybase annotation (http://flybase.org/). The ratio2 values for peptides mapped to the genes listed are indicated (ratio2 = average detection value experimental sample divided by average detection value control sample). *P*-values were obtained using the Student's *t*-test followed by multiple testing adjustment using the Benjamini–Hochberg method.[51]

persistent salivary gland fragments, 100% of those expressing *csn6-IR* in salivary glands contained persistent salivary gland fragments 24 h APF (Figures 4a and b). We identified csn6 as being enriched after proteasome inhibition. We tested if *csn6* is required for autophagy in dying salivary glands as altered proteasome function can lead to activation of autophagy in neurons,[34] however, knockdown of *csn6* did not influence autophagy (data not shown).

Discussion

Autophagic programmed cell death appears to be conserved between insects and mammals,[25,39] yet the mechanisms that contribute to this type of cell death are not well understood. We used a shotgun proteomic approach to identify proteins enriched during autophagic programmed cell death in purified dying *Drosophila* larval salivary glands. We found that a number of UPS components are enriched in dying salivary glands, suggesting a role for the UPS in salivary gland cell death. Significantly, UPS components are enriched in proteomic studies of apoptotic cells.[40] We tested the function of the UPS in salivary glands and found that flux through the UPS pathway is decreased during cell death in wild-type salivary glands.

Although the mechanism leading to decreased UPS function during salivary gland cell death remains unknown, it could be that UPS function is reduced by system overload, but other possibilities exist. It is interesting that a large number of UPS components are enriched in dying salivary glands at the time when UPS function is decreased, suggesting a possible compensatory upregulation to deal with a reduction in the function of this important catabolic process. We find that ectopic proteasome impairment leads to the onset of early salivary gland condensation and DNA fragmentation *in vivo*. Unexpectedly, however, we find that caspase inhibitor p35 expression during proteasome impairment does

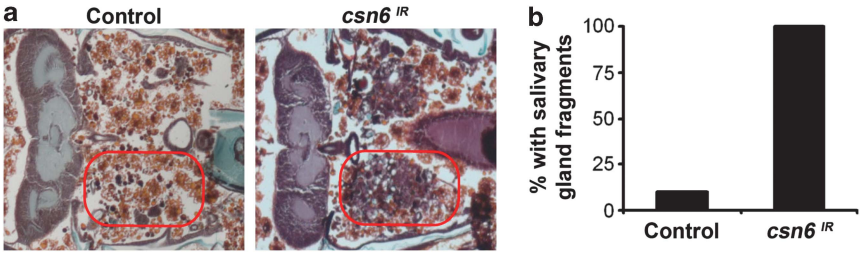

Figure 4 RNAi knockdown of CSN6 prevents salivary gland degradation. (**a**) Control animals lacking the GAL4 driver (+/w; +/UAS-*csn6*^{IR}), $n=10$, and those with salivary gland-specific knockdown of *csn6* (*fkh*-GAL4/w; UAS-*csn6*^{IR}/+), $n=22$, were analyzed by histology for the presence of salivary glands (red circles) 24 h AFP. *csn6*^{IR} = VDRC TID no. 22308 on II. (**b**) Quantification of data from (**a**) where 10% of control animals and 100% of experimental animals possess persistent salivary gland fragments

not suppress ectopic salivary gland condensation. This suggests that proteasome impairment-induced gland condensation may require the activity of caspase-independent processes.

We queried our proteomics data to identify factors present in salivary glands upon proteasome impairment. To identify physiologically relevant factors that might function in salivary gland cell degradation, we compared factors identified following ectopic proteasome impairment in salivary glands to those identified during wild-type salivary gland cell death. The simple presence of proteins in dying salivary glands is not evidence that these proteins function in cell death and degradation. Therefore, we took a genetic approach to screen top candidates for defects in salivary gland degradation by RNAi knockdown. Here, we show that the knockdown of *trol* and *CG11880*, a gene of unknown function, prevent proper salivary gland degradation. The gene *trol* has been shown to function in controlling the onset of stem cell proliferation in the developing *Drosophila* nervous system by modulating fibroblast growth factor branchless and Hedgehog signaling, and mutations in *trol* also affect Dpp and Wingless signaling.[41] However, neither *CG11880* nor *trol* has previously been shown to function in salivary gland cell degradation.

To identify additional genes that might function in autophagic cell death, we searched for proteins that are members of a pathway or cellular component and present during wild-type cell death and in response to proteasome impairment in salivary glands. We identified 7 out of 8 known CSN components by proteomics and demonstrated that RNAi knockdown of CSN subunit *csn6* prevents salivary gland degradation. The CSN is a conserved multi-subunit protein complex that functions in the ubiquitin/proteasome pathway.[42] First discovered in plants, the CSN is essential for *Drosophila* development and functions in a variety of essential cellular processes, including cell cycle control, the DNA-damage response, and circadian rhythm.[42] Composed of eight subunits, CSN1–CSN8, the CSN contains Nedd8 isopeptidase activity, and functions to remove the ubiquitin-like Nedd8 from proteins (deneddylate).[42]

Our finding that *csn6* is required for salivary gland degradation demonstrates a role for the CSN in autophagic cell death, and suggests that proper control of protein neddylation and deneddylation cycles is important to regulate salivary gland degradation. Several studies have demonstrated a role for the CSN in regulating cell death. *Csn5* knockout mice exhibit elevated apoptosis.[43,44] In addition, several cullin-RING ligase components negatively regulate *Caenorhabditis elegans* p53 (CEP-1)-dependent germ cell apoptosis in response to DNA damage.[45] Cullin-RING ligase complexes may also function in salivary gland cell death, a subject for future investigation.

Our proteomics analyses led to the discovery of several genes required for proper salivary gland cell degradation. These findings exhibit the power of a high-throughput proteomics approach to identify factors that function in biological processes. Our proteomics data will serve as a foundation for future genetic studies of autophagic programmed cell death and *in vivo* cellular responses to proteasome inhibition by providing a description of proteins enriched during wild-type cell death as well as in response to ectopic proteasome impairment.

Materials and Methods

***Drosophila* strains.** The Canton-S strain was used as wild-type. For ectopic proteasome impairment studies, UAS-Dts7^{2c} on III was used.[35] To monitor proteasome impairment, UAS-M-GFP was used as the positive control, and UAS-GFP-CL1 was used as the experimental stock.[32–34] For ectopic p35 expression, UAS-p35 was used.[46] The following Vienna *Drosophila* RNAi Center (VDRC, Vienna, Austria) RNAi stocks were used: *CG11880*^{IR} VDRC Transformant ID (TID) 22867 on II, *trol*^{IR} VDRC TID no. 245498 on II.

Proteomics analysis. To generate the proteomics data sets, at least three independent biological samples for each condition were collected. For each independent sample, 80 pairs of salivary glands were dissected per 100 μl 8 M urea/40 mM Tris-HCl, pH 8. At least two runs of each biological sample were analyzed, using 10 μg of sample per run, by high-throughput MS-based proteomics.[47] Proteins were fully trypsinized, and peptides were separated by two-dimensional chromatography; first into 15 fractions by capillary isoelectric focusing, and further resolved by capillary reverse-phase liquid chromatography (RPLC) (nano-RPLC). Two runs of each protein sample were carried out. Fractions were analyzed by ESI-tandem-MS using a Thermo Finnigan LTQ linear ion trap mass spectrometer (San Jose, CA, USA). Following MS analysis, peaklists were generated using extract_msn, and searches to identify MS/MS peptide spectra were carried out using the Open Mass Sepctrometry Search Algorithm[48] (NCBI). For each data set, protein and peptide hits were generated assuming a false positive rate of 5%, and proteins present in the samples were identified based upon peptide sequences detected. Comparison of proteomics data sets: Files containing flybase gene identifiers (FBGNs), flybase gene symbols, and RefSeq protein accession numbers were batch downloaded from http://www.flybase.org. Microsoft Access (Seattle, WA, USA) was then used to merge proteomics data files with that containing FBGN, flybase gene symbols, and RefSeq accessions. Using Microsoft Access, separate proteomics data sets containing ratio2 values were then merged based upon their common FBGN numbers. This allowed the comparison of ratio2 values and *P*-values between proteins identified in more than one proteomics data set.

Histology. Histology was performed as previously described.[49]

Protein extracts and western blotting. Protein extraction and western blotting were performed as previously described.[50] Primary antibodies used were rabbit anti-ubiquitin (1 : 1000), and mouse anti-beta-tubulin (1 : 50; z).

Microscopy. Imaging was performed on a Zeiss (New York, NY, USA) Axiophot II microscope. To quantify salivary gland size, the area of the largest salivary gland section per pupa was measured using the Zeiss AxioVisionLE software.

Conflict of Interest

The authors declare no conflict of interest.

Acknowledgements. We thank P Meier, the Bloomington Stock Center, and the VDRC for *Drosophila* strains. We thank K Simin for assistance with proteomics data analysis. This work was supported by the NIH grant GM079431 to EHB. EHB is an Ellison Medical Foundation Scholar and a member of the UMass DERC (DK32520).

1. Lockshin RA, Williams CM. Programmed cell death-I. Cytology of degeneration in the intersegmental muscles of the pernyi silkmoth. *J Insect Physiol* 1965; **11**: 123–133.
2. Danial NN, Korsmeyer SJ. Cell death: critical control points. *Cell* 2004; **116**: 205–219.
3. Thompson CB. Apoptosis in the pathogenesis and treatment of disease. *Science* 1995; **267**: 1456–1462.
4. Clarke PGH. Developmental cell death: morphological diversity and multiple mechanisms. *Anat Embryol* 1990; **181**: 195–213.
5. Schweichel J-U, Merker H-J. The morphology of various types of cell death in prenatal tissues. *Teratology* 1973; **7**: 253–266.
6. Ciechanover A. Proteolysis: from the lysosome to ubiquitin and the proteasome. *Nat Rev Mol Cell Biol* 2005; **6**: 79–87.
7. Schwartz AL, Ciechanover A. The ubiquitin-proteasome pathway and pathogenesis of human diseases. *Annu Rev Med* 1999; **50**: 57–74.
8. Wang J, Maldonado MA. The ubiquitin-proteasome system and its role in inflammatory and autoimmune diseases. *Cell Mol Immunol* 2006; **3**: 255–261.
9. Drexler HC. Programmed cell death and the proteasome. *Apoptosis* 1998; **3**: 1–7.
10. Sun XM, Butterworth M, MacFarlane M, Dubiel W, Ciechanover A, Cohen GM. Caspase activation inhibits proteasome function during apoptosis. *Mol Cell* 2004; **14**: 81–93.
11. Adrain C, Creagh EM, Cullen SP, Martin SJ. Caspase-dependent inactivation of proteasome function during programmed cell death in Drosophila and man. *J Biol Chem* 2004; **279**: 36923–36930.
12. Schwartz LM, Myer A, Kosz L, Engelstein M, Maier C. Activation of polyubiquitin gene expression during developmentally programmed cell death. *Neuron* 1990; **5**: 411–419.
13. Jones ME, Haire MF, Kloetzel PM, Mykles DL, Schwartz LM. Changes in the structure and function of the multicatalytic proteinase (proteasome) during programmed cell death in the intersegmental muscles of the hawkmoth, Manduca sexta. *Dev Biol* 1995; **169**: 436–447.
14. Dawson SP, Arnold JE, Mayer NJ, Reynolds SE, Billett MA, Gordon C *et al.* Developmental changes of the 26 S proteasome in abdominal intersegmental muscles of Manduca sexta during programmed cell death. *J Biol Chem* 1995; **270**: 1850–1858.
15. Takayanagi K, Dawson S, Reynolds SE, Mayer RJ. Specific developmental changes in the regulatory subunits of the 26 S proteasome in intersegmental muscles preceding eclosion in Manduca sexta. *Biochem Biophys Res Commun* 1996; **228**: 517–523.
16. Shinohara K, Tomioka M, Nakano H, Tone S, Ito H, Kawashima S. Apoptosis induction resulting from proteasome inhibition. *Biochem J* 1996; **317**(Part 2): 385–388.
17. Drexler HC. Activation of the cell death program by inhibition of proteasome function. *Proc Natl Acad Sci USA* 1997; **94**: 855–860.
18. Henderson CJ, Aleo E, Fontanini A, Maestro R, Paroni G, Brancolini C. Caspase activation and apoptosis in response to proteasome inhibitors. *Cell Death Differ* 2005; **12**: 1240–1254.
19. Hoeller D, Dikic I. Targeting the ubiquitin system in cancer therapy. *Nature* 2009; **458**: 438–444.
20. Tobinai K. Proteasome inhibitor, bortezomib, for myeloma and lymphoma. *Int J Clin Oncol* 2007; **12**: 318–326.
21. Adams J. The development of proteasome inhibitors as anticancer drugs. *Cancer Cell* 2004; **5**: 417–421.
22. Ling YH, Liebes L, Jiang JD, Holland JF, Elliott PJ, Adams J *et al.* Mechanisms of proteasome inhibitor PS-341-induced G(2)-M-phase arrest and apoptosis in human non-small cell lung cancer cell lines. *Clin Cancer Res* 2003; **9**: 1145–1154.
23. Meister S, Schubert U, Neubert K, Herrmann K, Burger R, Gramatzki M *et al.* Extensive immunoglobulin production sensitizes myeloma cells for proteasome inhibition. *Cancer Res* 2007; **67**: 1783–1792.
24. Gu H, Chen X, Gao G, Dong H. Caspase-2 functions upstream of mitochondria in endoplasmic reticulum stress-induced apoptosis by bortezomib in human myeloma cells. *Mol Cancer Ther* 2008; **7**: 2298–2307.
25. Berry DL, Baehrecke EH. Growth arrest and autophagy are required for salivary gland cell degradation in Drosophila. *Cell* 2007; **131**: 1137–1148.
26. Lee C-Y, Baehrecke EH. Steroid regulation of autophagic programmed cell death during development. *Development* 2001; **128**: 1443–1455.
27. Martin DN, Baehrecke EH. Caspases function in autophagic cell death in Drosophila. *Development* 2004; **131**: 275–284.
28. Lee C-Y, Clough EA, Yellon P, Teslovich TM, Stephan DA, Baehrecke EH. Genome-wide analyses of steroid- and radiation-triggered programmed cell death in Drosophila. *Curr Biol* 2003; **13**: 350–357.
29. Martin DN, Balgley B, Dutta S, Chen J, Rudnick P, Cranford J *et al.* Proteomic analysis of steroid-triggered autophagic programmed cell death during Drosophila development. *Cell Death Differ* 2007; **14**: 916–923.
30. Lee CY, Wendel DP, Reid P, Lam G, Thummel CS, Baehrecke EH. E93 directs steroid-triggered programmed cell death in Drosophila. *Mol Cell* 2000; **6**: 433–443.
31. Yao T-P, Forman BM, Jiang Z, Cherbas L, Chen JD, McKeown M *et al.* Functional ecdysone receptor is the product of EcR and ultraspiracle genes. *Nature* 1993; **366**: 476–479.
32. Dantuma NP, Lindsten K, Glas R, Jellne M, Masucci MG. Short-lived green fluorescent proteins for quantifying ubiquitin/proteasome-dependent proteolysis in living cells. *Nat Biotechnol* 2000; **18**: 538–543.
33. Bence NF, Bennett EJ, Kopito RR. Application and analysis of the GFPu family of ubiquitin-proteasome system reporters. *Methods Enzymol* 2005; **399**: 481–490.
34. Pandey UB, Nie Z, Batlevi Y, McCray BA, Ritson GP, Nedelsky NB *et al.* HDAC6 rescues neurodegeneration and provides an essential link between autophagy and the UPS. *Nature* 2007; **447**: 859–863.
35. Belote JM, Fortier E. Targeted expression of dominant negative proteasome mutants in Drosophila melanogaster. *Genesis* 2002; **34**: 80–82.
36. Busch S, Schwier EU, Nahlik K, Bayram O, Helmstaedt K, Draht OW *et al.* An eight-subunit COP9 signalosome with an intact JAMM motif is required for fungal fruit body formation. *Proc Natl Acad Sci USA* 2007; **104**: 8089–8094.
37. Serino G, Deng XW. The COP9 signalosome: regulating plant development through the control of proteolysis. *Annu Rev Plant Biol* 2003; **54**: 165–182.
38. Su H, Huang W, Wang X. The COP9 signalosome negatively regulates proteasome proteolytic function and is essential to transcription. *Int J Biochem Cell Biol* 2009; **41**: 615–624.
39. Elgendy M, Sheridan C, Brumatti G, Martin SJ. Oncogenic Ras-induced expression of Noxa and Beclin-1 promotes autophagic cell death and limits clonogenic survival. *Mol Cell* 2011; **42**: 23–35.
40. Arntzen MØ, Thiede B. ApoptoProteomics an integrated database for analysis of proteomics data obtained from apoptotic cells. *Mol Cell Proteomics* 2012; **11,** M111.010447.
41. Lindner JR, Hillman PR, Barrett AL, Jackson MC, Perry TL, Park Y *et al.* The Drosophila Perlecan gene trol regulates multiple signaling pathways in different developmental contexts. *BMC Dev Biol* 2007; **7**: 121.
42. Wei N, Serino G, Deng XW. The COP9 signalosome: more than a protease. *Trends Biochem Sci* 2008; **33**: 592–600.
43. Tomoda K, Yoneda-Kato N, Fukumoto A, Yamanaka S, Kato JY. Multiple functions of Jab1 are required for early embryonic development and growth potential in mice. *J Biol Chem* 2004; **279**: 43013–43018.
44. Panattoni M, Sanvito F, Basso V, Doglioni C, Casorati G, Montini E *et al.* Targeted inactivation of the COP9 signalosome impairs multiple stages of T cell development. *J Exp Med* 2008; **205**: 465–477.
45. Gao MX, Liao EH, Yu B, Wang Y, Zhen M, Derry WB. The SCF FSN-1 ubiquitin ligase controls germline apoptosis through CEP-1/p53 in *C. elegans*. *Cell Death Differ* 2008; **15**: 1054–1062.
46. Hay BA, Wolff T, Rubin GM. Expression of baculovirus P35 prevents cell death in Drosophila. *Development* 1994; **120**: 2121–2129.
47. Chen J, Balgley BM, DeVoe DL, Lee CS. Capillary isoelectric focusing-based multidimensional concentration/separation platform for proteome analysis. *Anal Chem* 2003; **75**: 3145–3152.
48. Geer LY, Markey SP, Kowalak JA, Wagner L, Xu M, Maynard DM *et al.* Open mass spectrometry search algorithm. *J Proteome Res* 2004; **3**: 958–964.
49. Muro I, Berry DL, Huh JR, Chen CH, Huang H, Yoo SJ *et al.* The Drosophila caspase Ice is important for many apoptotic cell deaths and for spermatid individualization, a nonapoptotic process. *Development* 2006; **133**: 3305–3315.
50. Dutta S, Baehrecke EH. Warts is required for PI3K-regulated growth arrest, autophagy, and autophagic cell death in Drosophila. *Curr Biol* 2008; **18**: 1466–1475.
51. Hochberg Y, Benjamini Y. More powerful procedures for multiple significance testing. *Stat Med* 1990; **9**: 811–818.

Supplementary information accompanies the paper on Cell Death and Differentiation website (http://www.nature.com/cdd)